International Journal of GEOMATE, Jan., 2020, Vol.18, Issue 65, pp. 1 - 8
ISSN: 2186-2982 (P), 2186-2990 (O), Japan, DOI: https://doi.org/10.21660/2020.65.5558
Geotechnique, Construction Materials and Environment

STRESS ANALYSIS OF EMBANKMENT DUE TO DIFFERENT IN CONSTRUCTION CONDITIONS

*Shin-ichi Kanazawa[1] and Satoe Suzuki[2]

[1]Civil and environmental engineering, National Institute of Technology, Fukushima College, Japan
[2]National Institute of Technology, Fukushima College, Japan

*Corresponding Author, Received: 26 Oct. 2019, Revised: 19 Nov. 2019, Accepted: 10 Dec. 2019

ABSTRACT: In recent years, many examples of soil structure collapse due to heavy rainfall have occurred. Because of this, it is urgent to establish a method to evaluate and examine long-term embankment structure quality. Japan's conventional design method insufficiently evaluates embankments. Although this method is shifting to a performance-based design to cope with recent abnormal weather, an effective design method has not yet been established. Therefore, this research performs an initial stress analysis of embankment, accounting for differences in construction conditions. Notable in this study, is the comparative analysis of results, considering the initial water content ratio, one layer of discharge thickness, rolling compaction, and other given structural conditions that differed from conventional design standards. To do this, first the initial moisture content ratio was determined by reproducing the compaction by analysis. Second, based on the dynamics of unsaturated soil, the rainfall intensity was analyzed in order to confirm the variation of the initial stress due to rainfall. Lastly, and most critically, the dynamic change in embankment performance was analytically expressed, and the optimal structural conditions of embankment, grouped by rainfall history, was examined.

Keywords: Embankment, Unsaturated soil, Construction condition, Compaction, Finite element analysis

1. INTRODUCTION

Soil compaction tests are carried out to improve embankment construction engineering characteristics, such as stability and deformation. In selecting the soil compaction level to use at a construction site, the water ratio (optimum water ratio) is necessary. This is most efficiently obtained from the relationship between the dry density and the water content of the soil for compaction by changing the water content of soil. From this, the soil structure is constructed using the compaction soil. In recent years, however, many cases of embankment collapse have been reported in Japan due to excessive rainfall and torrential downpours caused by typhoons. Take for example, the torrential rain in the northern part of Kyushu in July 2017 and typhoon No. 18 that hit the Kanto and Tohoku regions in 2015. The river embankments and roads collapsed, and a landslide on the general national highway occurred due to the record heavy rain. At present, the mechanisms of embankment collapse due to such natural disasters are not sufficiently clarified. According to guidelines, the stability of embankment against heavy rain is strongly dependent on four factors: treatment of the underlying ground, quality of embankment material, degree of compaction, and drainage. There are many cases where a drainage issue, in particular, has led to embankment collapse. It is worth mentioning that the construction and maintenance of embankment is developed based on empirical engineering rules and that the strength of embankment is lowered by intermittent heavy rain. The soil is composed of three phases: solid, liquid, and air. Embankment soil below the groundwater level often exists in the unsaturated state containing air or dissolved air. As pore air pressure changes due to rainfall infiltration, the dissolution and release of air into the liquid phase occurs, seeming to compress the soil volume. As a result of not accounting for this factor, present construction guidelines may not provide sufficient embankment drainage countermeasures for the concentrated rain observed of late, coupled with the given construction compaction management. Furthermore, the civil engineering evaluation of performance-based design, essential to meeting the required performance of engineered structures, is also changing. When an earthquake struck Hyogo Prefecture in 1995, many buildings escaped destruction but became unusable. This is because performance-based design, in which the performance for the assumed load is considered during design, was not sufficiently implemented. Taking this type of disaster as an opportunity for change, structural plans and details have been developed for soil structures, shifting the field to performance-based design to ensure that the required performance is satisfied throughout the service life of the design. It is urgent to establish the techniques that can evaluate and examine the

long-term quality of embankment structures and what elements of performance design will be important in the future. Based on the above, this study attempted to analyze the effects of rainfall intensity to grasp the fluctuation due to rainfall of each initial stress, based on the dynamics of unsaturated soil. In addition, changes in the dynamic behavior of the embankment were expressed analytically, and the optimum construction condition for embankment structure at a given to rainfall history were investigated.

2. MATHEMATICAL MODEL USED FOR SOIL/WATER/AIR COUPLED FINITE ELEMENT ANALYSIS

The finite element analysis code [1] (DACSAR-MP) used in this study formulates the unsaturated soil constitutive model proposed by Ohno et al [2]. This model is framed as the soil/water/air coupled problem using the three-phase mixture theory. This study proposes a model in which the effective degree of saturation is used as the state quantity to represent rigidity, by referring to the model of Karube et al., which defines effective stress considering water content [3]. Equation (1) shows the effective stress. Equation (2) shows the base stress tensor and suction stress. Equation (3) shows suction.

$$\boldsymbol{\sigma}' = \boldsymbol{\sigma}^{\mathbf{net}} + p_s \mathbf{1} \tag{1}$$

$$\boldsymbol{\sigma}^{\mathbf{net}} = \boldsymbol{\sigma} - p_a \mathbf{1}, \;\; p_s = S_e s \tag{2}$$

$$s = p_a - p_w, S_e = \frac{S_r - S_{rc}}{1 - S_{rc}} \tag{3}$$

Here, $\boldsymbol{\sigma}'$ is the effective stress tensor; $\boldsymbol{\sigma}^{\mathbf{net}}$ is the base stress tensor; $\mathbf{1}$ is the second order unit tensor; $\boldsymbol{\sigma}$ is the total stress tensor; s is the suction; p_s is the suction stress; p_a is the pore air pressure; p_w is the pore water pressure; S_r is the degree of saturation; S_e is the effective degree of saturation; and S_{rc} is the degree of saturation at s→∞. In numerical calculations, the EC model of Ohno et al. [4], which does not have a singularity in the yield surface, was incorporated to avoid shifting to the singularity, a quantity impossible to differentiate, during preconsolidation pressure at saturation. Equations (4), (5), (6) and (7) were expressed to provide the yield function of unsaturated soil.

$$f\left(\boldsymbol{\sigma}', \zeta, \varepsilon_v^p\right) = MD \ln \frac{p'}{\zeta p_{sat}'} + \frac{MD}{n_E}\left(\frac{q}{Mp'}\right)^{n_E} - \varepsilon_v^p = 0 \tag{4}$$

$$\zeta = \exp\left[\left(1 - S_e\right)^{n_s} \ln a\right], MD = \frac{\lambda - \kappa}{1 + e_0} \tag{5}$$

$$p' = \frac{1}{3}\boldsymbol{\sigma}' : \mathbf{1}, q = \sqrt{\frac{3}{2}\mathbf{s} : \mathbf{s}} \tag{6}$$

$$\mathbf{s} = \boldsymbol{\sigma}' - p'\mathbf{1} = \mathbf{A} : \boldsymbol{\sigma}', \mathbf{A} = \mathbf{I} - \frac{1}{3}\mathbf{1} \otimes \mathbf{1} \tag{7}$$

Here, n_E is the shape parameter; ε_v^p is the plastic volume strain; M is the *q/p'* in the limit state; D is the dilatancy coefficient; p_{sat}' is the yield stress at saturation; a and n_s are the parameters representing the increase in yield stress due to unsaturation; λ is the compression index; and κ is the expansion index. Equation (8) shows pore water velocity. Equation (9) shows air velocity. Pore water and air flow follow Darcy's law.

$$\tilde{v}_{\mathrm{w}} = -\mathbf{k}_{\mathbf{w}} \cdot \mathrm{grad} h \tag{8}$$

$$\tilde{v}_{\mathrm{a}} = -\mathbf{k}_{\mathbf{a}} \cdot \mathrm{grad} h_a, h_a = \frac{p_a}{\gamma_w} \tag{9}$$

Here, $\tilde{v}_{\mathrm{w}}$ is the pore water velocity; $\tilde{v}_{\mathrm{a}}$ is the air velocity; $\mathbf{k}_{\mathbf{w}}$ is the hydraulic conductivity; $\mathbf{k}_{\mathbf{a}}$ is the coefficient of air permeability; h is the total head; γ_w is the unit weight of water; and h_a is the pneumatic head. Equations (10)-(11) show hydraulic conductivity and the coefficient of air permeability by way of Mualem's [5] formula and the Van Genuchten [6] formula.

$$\mathbf{k}_{\mathbf{w}} = k_{rw}\mathbf{k}_{\mathbf{wsat}} = S_e^{1/2}\left[1 - \left(1 - S_e^{1/m}\right)^m\right]^2 \mathbf{k}_{\mathbf{wsat}} \tag{10}$$

$$\mathbf{k}_{\mathbf{a}} = k_{ra}\mathbf{k}_{\mathbf{ares}} = \left(1 - S_e\right)^{1/2}\left(1 - S_e^{1/m}\right)^{2m} \mathbf{k}_{\mathbf{ares}} \tag{11}$$

Here, k_{rw} is the ratio of hydraulic conductivity; k_{ra} is the ratio of coefficient of air permeability; m is the Mualem constant; $\mathbf{k}_{\mathbf{wsat}}$ is the hydraulic conductivity at saturation; $\mathbf{k}_{\mathbf{ares}}$ is the coefficient of air permeability in dry conditions. Equations (12)-(13) show the continuous formula of pore water and air using three-phase mixture

theory.

$$n\dot{S}_r - S_r\dot{\varepsilon}_v + \mathrm{div}\tilde{v}_w = 0 \quad (12)$$

$$(1-S_r)\dot{\varepsilon}_v + n\dot{S}_r - n(1-S_r)\frac{\dot{p}_a}{p_a + p_0} - \mathrm{div}\tilde{v}_a = 0 \quad (13)$$

Here, n is porosity; $\dot{\varepsilon}_v$ is volumetric strain; and p_0 is atmospheric pressure. The elasto-plastic constitutive model obtained from Equation (4) and the equilibrium equation [Equations (12) - (13)] are formulated as the soil/water/air coupled problem.

3. REPRODUCTION OF COMPACTION BY ANALYSIS

3.1 Moisture Characteristic Curve Used In The Analysis

For a soil-water characteristic curve model, a model capable of hysteresis expression, as proposed by Kawai et al. [7], is used. In addition, to determine the logistic curve in the case of DRY and WET, derived from arbitrary suction and the degree of saturation, the logistic curve equation of Sugii and Uno [8] was used. This makes it possible to grasp the moisture conditions of sloped ground where complex water balance occurs. Figure 1 exhibits the soil-water characteristic curve used in this study. Here, A and B are fitting parameters of the water characteristic curve. The suffix D shows a logistic curve in the case of DRY and W shows a logistic curve in the case of WET.

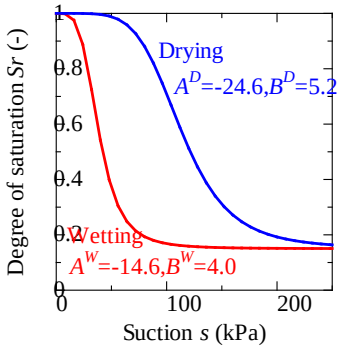

Fig. 1 Soil water characteristic curve

3.2 Summary of Analysis Condition

In this study, embankment analysis considering compaction was carried out using the unsaturated soil/water/air coupled finite element analysis code (DACSAR-MP). In addition, rainfall and evapotranspiration conditions, as well as different construction conditions were applied to the initial stress analysis. Initial stress in this study indicates the stress state at completion of embankment construction. Table 1 shows material parameters. Material parameters were determined considering the results of previous studies by Honda et al. [9]. Here, λ is the compression index; κ is the swelling index; m is the unsaturated permeability coefficient of Mualem; k_a is the coefficient of air permeability; k_w is the hydraulic conductivity; e_0 is the initial void ratio; S_{r0} is the critical degree of saturation; a is the parameter that determines the magnification of consolidation yield stress at its maximum by increasing stiffness due to desaturation; and V is Poisson's ratio.

Table 1 Material parameters

λ	κ	M	m	S_{r0}	k_a(m/day)	p'_{sat}(kPa)
0.13	0.013	1.33	0.8	0.15	1.0	20.0
n	n_E	a	v	G_s	k_w(m/day)	e_0
1.0	1.3	10.0	0.33	2.7	0.01	1.0

Using these parameters, a compaction test simulating a 13cm high × 10cm wide mold was analytically conducted to grasp the optimum moisture content of silt-mixed soil. Fig. 2 shows the analysis domain. The upper, lower, left, and right hydraulic boundaries shall be undrained. The displacement boundary was fixed vertically at the lower end and horizontally at the upper end, and plane strain analysis was carried out. The following are the analysis conditions. The initial water content ratio was set to w = 10 to 28% at a 2% interval and a total of 10 cases were considered. The loading was set at 500kPa, and the time required for loading and unloading was set at 1 minute. Figure 3 shows the loading conditions.

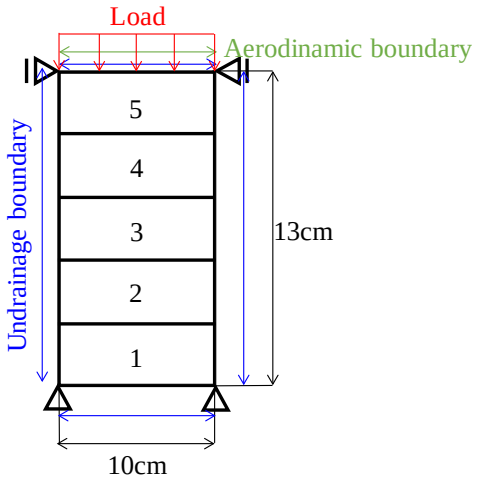

Fig. 2 Analysis domain

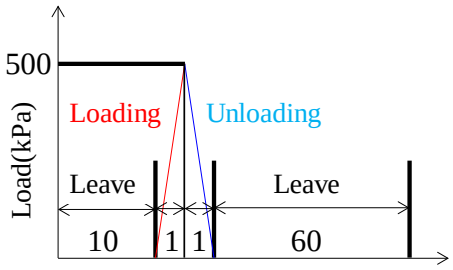

Fig. 3 Loading conditions

3.3 Analyses Results

From the compaction curve shown in Figure 4, the optimum water content was obtained as w = 18%. Since the compacted embankment was unsaturated during construction, the force between soil particles was generated by the suction caused by the surface tension of water. However, suction disappeared when the embankment approached a saturation state due to rainfall after the banking was completed. In the case of soil with a large void ratio, volume decrease (settlement) by overloading and strength decrease may correspond to the lowering of the interparticle force. This phenomenon is apt to occur on the dry side of the embankment where the water content is low and where the optimum water content, or the slightly wet side water content, is adopted in construction. In addition, the water content near the optimum water content obtained by the standard test can be used at the construction site according to the method regulation described in the guideline of road construction and embankment construction [10]. Therefore, by using three water content ratios of w = 18%, w = 16% and w = 20% (corresponding to w_{opt} ± 2% located near the optimum water content), the embankment analysis described in the next chapter was conducted, and the stress behavior was compared.

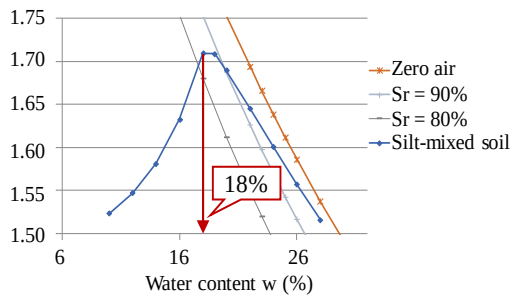

Fig. 4 Compaction curve

4. REPRODUCTION OF EMBANKMENT CONSTRUCTION PROCESSES BY NUMERICAL ANALYSIS

4.1 Analysis Condition

4.1.1 Conditions of boundaries

Figure 5 shows the analysis mesh. The three water content ratios obtained from Figure 4 in the previous section were used as the initial water contents for analyzing embankments with construction conditions that differed from convention. The analysis region is assumed to be the foundation ground of 15m in length and 45m in width, and the banking of 3m in crest width, 15m in lower end and 6m in height. The compaction is expressed by carrying out loading and unloading to each layer under a loading condition of 500kPa After the layer is rolled out for 0.3m. For the displacement boundary, the lower end of the foundation ground is fixed vertically and horizontally, and plane strain analysis is carried out. The upper, lower, left, and right hydraulic boundaries shall be undrained. The foundation soil shall be saturated to a depth of 3m or more from the ground surface. The soil-water characteristic curve used for the embankment analysis in the previous section was again employed.

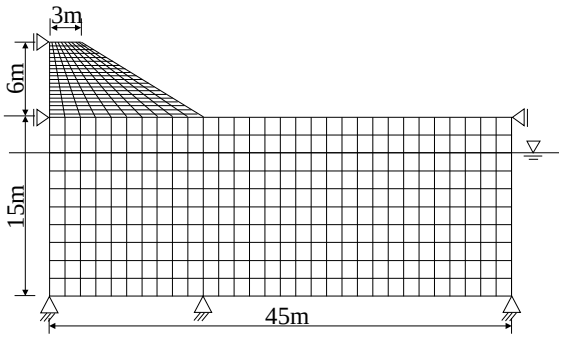

Fig. 5 Analysis mesh

4.1.2 Construction process

Figure 6 shows the flow of the embankment construction process. When forming the element, a predetermined head for each layer is given as an initial condition. At the node that is in contact with the atmosphere, the water is not drained. The water balance is generated by the applied head, and a new head is calculated. The same procedure is also applied when the element is placed on top of it. Between the piled layer and its lower layer, the condition changes from non-drainage condition to drainage condition to enable water balance between upper and lower elements.

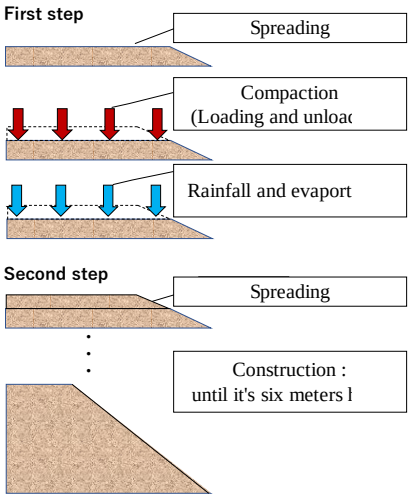

Fig. 6 The flow of embankment construction process

Figure 7 shows the analysis steps used to complete the embankment. The analysis step consists of one layer winding, then loading. Considering that the water balance between the layers sufficiently reaches a steady state for parameters such as permeability and others during unloading, rainfall and evaporation, each period is set to 1 day.

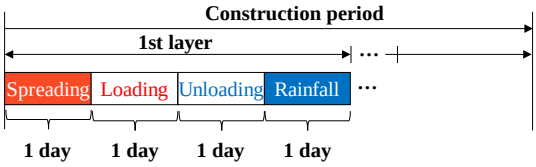

Fig.7 The analysis steps used to complete the embankment

4.1.3 Summary of rainfall and evaporation

Rainfall history was based on 2005 annual rainfall (1784mm) and evaporation (324mm) in Hikone City, Shiga Prefecture [10] to simulate the average rainfall in Japan.

4.1.4 Construction conditions

The analysis condition was set at a rolling compaction strength of 500kPa after a layer of 0.3m of spreading. The compaction was reproduced by statically loading and unloading each layer. The plane strain analysis was carried out on the displacement boundary with the lower end of the foundation soil fixed vertically and horizontally. The hydraulic boundary is set to an undrained condition above, below, and to the left and right. The above analysis condition is referred to as Case 1. It is assumed to be a conventional construction method. Case 2 is an analysis condition in which the spreading lift of one layer is changed from 0.3m to 0.5m. In addition, the embankment analysis was also carried out under the conditions of Case 3, in which the spreading lift of one layer was changed to 0.6m. Table 2 shows construction conditions (Case1 through Case3).

Table2 Construction conditions (Case1-3)

	Case1	Case2	Case3
Spreading lift	0.3m	0.5m	0.6m
Compaction speed	0.3m/day	0.5m/day	0.6m/day

The above construction conditions used in Cases 1-3 are assumed as conventional construction conditions. The conditions in Cases 4-6, in which only the compaction speed was doubled, were assumed. In addition, the construction conditions as conventional construction are Case1 only, and Case2-Case6 change construction conditions from the conventional construction. Table 3 shows construction conditions (Case4 through Case6). Analysis was carried out considering construction conditions for a total of 6 cases.

Table 3 Construction conditions (Case4-6)

	Case4	Case5	Case6
Spreading lift	0.3m	0.5m	0.6m
Compaction speed	0.6m/day	1.0m/day	1.2m/day

4.2 Analyses Results

No large difference in stress change for the foundation soil in any of the analytical conditions occurred, but the stress change of the embankment division is apparent.

Figure 8 shows the effective stress under normal construction conditions, and Figure 9 shows the void ratio, also under normal construction conditions.

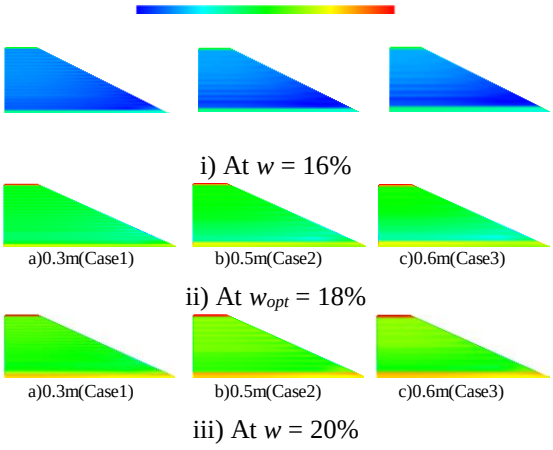

Fig. 8 Normal construction (Effective stress)

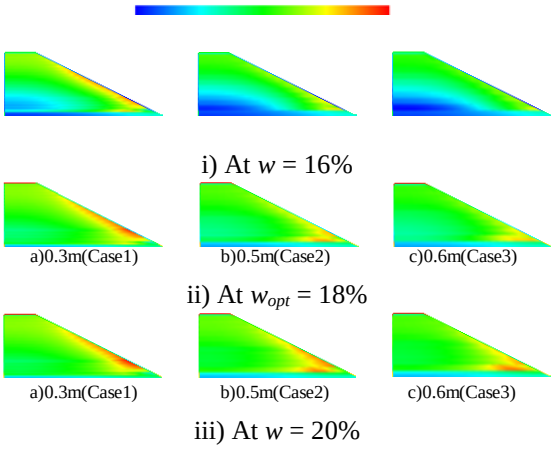

Fig. 9 Normal construction (Void ratio)

Comparing the results of Figures 8 and 9 shows that the distribution of effective stress and the void ratio under normal construction (Case 1 through Case 3) at the optimum moisture content (w_{opt} = 18%) expands at the surface of the embankment, and the value of the effective stress tends to decrease when the spreading lift of one layer was 0.3m. Furthermore, as the thickness of each layer is increased from 0.3m to 0.5m and 0.6m, it expands toward the toe of the slope, and the effective stress tended to decrease. Since the rolling strength of compaction was unified to 500kPa, it is thought that the rolling compaction was not sufficiently transmitted to the soil as the thickness of one layer gradually increased from 0.3m to 0.5m and 0.6m. This was likely caused by the difficulty of air discharging from the soil. Results from the embankment with water content w = 20% show the same tendency as the embankment with the optimum moisture content. the consolidation effect in the embankment was demonstrated, and the part which shows the expansion tendency tended to be distributed most widely as the thickness of one layer increased. Furthermore, the effective stress of embankment is low when the water content is 16%, the effective stress showed low value, and the void ratio concentrated in the embankment surface layer and showed the expansion tendency. The reason why the effective stress tended to be low is considered to be the decrease of suction by rainfall infiltration and the increase of pore water pressure.

Figure 10 shows the distribution of effective stress under the shortened construction period, and Figure 11 shows the distribution of void ratio under the shortened construction period. The tendency mentioned above is also observed in the analysis of a construction period shortened from the conventional time period (change of compaction speed to twice that of normal compaction).

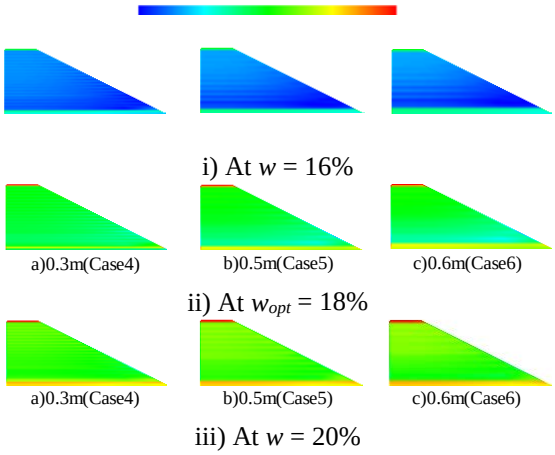

Fig. 10 Shortening of construction period (Effective stress)

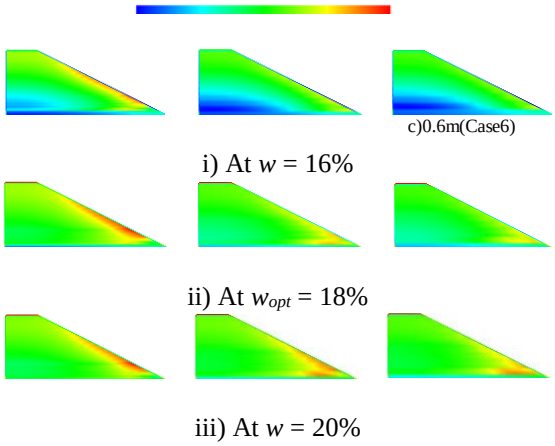

Fig. 11 Shortening of construction period (Void ratio)

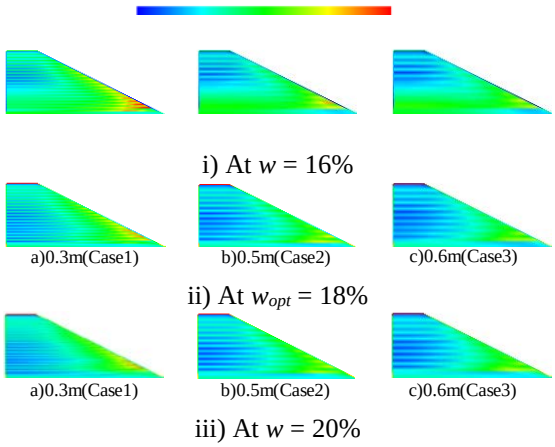

Fig. 12 Normal construction (Shear strain)

Figure 12 shows the distribution of shear strain under normal construction conditions. The results

of embankment analysis using the optimum water content (w = 18%) as the initial water content show that shear strain predominantly occurs from the surface to the tip of the embankment when the thickness of one layer was 0.3m (Case 1). Case 1 is most likely to demonstrate the compaction effect, because the layer thickness is thinner than other construction conditions. Since sand is used for the embankment material, drainage is higher than when silt or viscous soil are used. It is thought that this result is obtained because drainage water flows easily in the embankment surface layer. In the case of the construction condition in which one layer's spreading lift was 0.3m, drainage water concentrates in the tip due to the height of drainage. From these results, the compaction effect is easily detected. When the spreading lift of each layer was changed from 0.3m to 0.5m and 0.6m, the shear strain appears predominantly inside the embankment, not in the surface layer. Results for embankment with other water contents (w = 16%, w = 20%) shows the same tendency. This can be due to the fact that the compaction effect decreases as the layer thickness increases because the rolling compaction was kept constant.

Additionally, Figure 13 shows the distribution of shear strain when the construction period was shortened to half the normal time period (twice the compaction speed of normal construction).

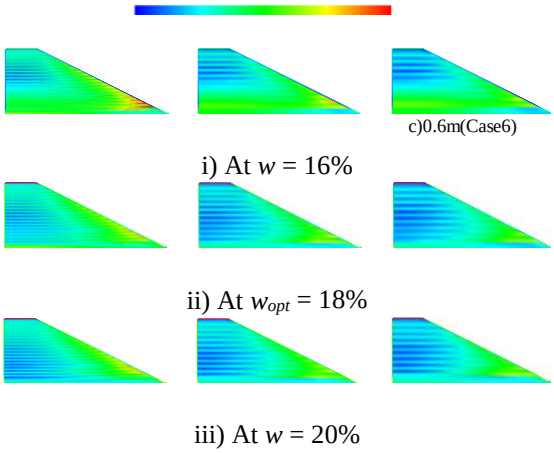

Fig. 13 Shortening of construction period (Shear strain)

In comparing the results from Figures 9 and 10, the distribution of embankment shear strain in Cases 5 and 6 is slightly larger than for embankment under normal construction. It is likely that the rolling strength was not well transmitted to the soil and the inside of the embankment was not sufficiently compacted with thicknesses increasing 0.3m to 0.5m and 0.6m when the compaction speed increased.

Figure 14 shows the critical condition judgement ratio for normal construction.

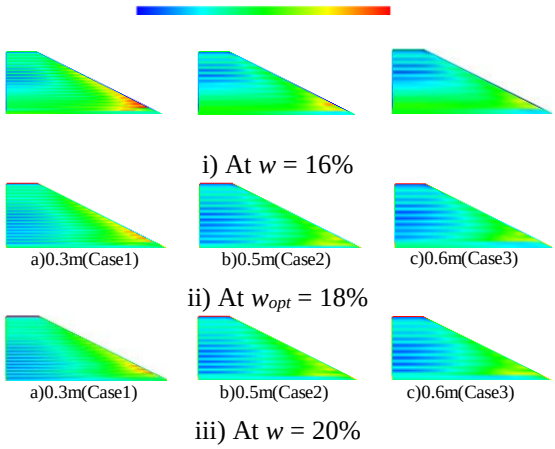

Fig. 14 Normal construction (Critical condition judgement ratio)

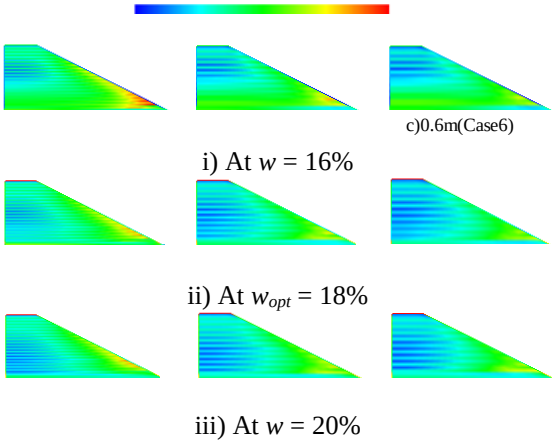

Fig. 15 Shortening of construction period (Critical condition judgement ratio)

The critical condition judgment ratio is an index indicating the possibility of destruction of a structure due to low stability when the maximum value exceeds 1.33.

In Case 1, the results of embankment analysis using the optimum water content as the initial water content shows excellent values from the surface to the tip of the embankment. The maximum value of 0.283 is not large enough to indicate destruction in the analytical result of this study, but it does indicate that surface layer slip may occur depending on future environmental changes at the periphery of the embankment. Case 2 and Case 3 also shows a similar tendency, and it seems that the toe of the embankment slope becomes weak at the time of embankment completion.

The results of the embankment analysis using w = 16% and w = 20% as the initial water content are similar to those of embankments with optimum

water content.

Furthermore, Figure 15 shows the critical condition judgment ratio in the case of shortening the construction period to half of the normal construction time period. A comparison between Figure 14 and Figure 15 shows that there is no significant difference in performance even if the construction period is shortened, as the same tendency is observed in all analytical conditions.

5. CONCLUSIONS

In this study, by using unsaturated soil/water/air coupled finite element analysis, embankment analysis considering compaction, rainfall, evaporation and various construction conditions was conducted, and the change of stress behavior in the embankment was expressed analytically. Resultingly, the optimum construction condition was examined. The results are summarized below. From the compaction test on the embankment, a numerical analysis was used to solve the embankment continuously. The numerical analysis is considered as one of the possible indices to evaluate the performance of the embankment in the long term.

The validity of conventional construction was confirmed by numerical analysis of the embankment structure, assuming various construction conditions. Since samples and natural field environments vary, a result validating the usefulness of future analysis techniques was obtained by reproducing various construction conditions by analysis. In the future, more precise and higher quality evaluations will be possible by analyzing the in-service process. The behavior of embankment is greatly changed by rainfall history and other factors, and at this time, this study's conclusions are limited to the very ideal conditions in this analysis. In the future, it is necessary to carry out the analysis under conditions closer to the natural environment.

6. REFERENCES

[1] Kanazawa, S., Toyoshima, K., Kawai, K., Tachibana, S. and Iizuka, A.: Analysis of mechanical behavior of compacted soil with F.E. method, journal of JSCE, No.68 (2), pp.291-298, 2012.

[2] Ohno, S., Kawai, K. and Tachibana, S.: Elasto-plastic constitutive model for unsaturated soil applied effective degree of saturation as a parameter expressing stiffness, Journal of JSCE, Vol.63/No.4, pp.1132-1141,2007.

[3] Karube D., Kato S., Hamada K. and Honda M.: The relationship between the mechanical behavior and the state of porewater in unsaturated soil, Journal of JSCE, No. 535/III-34, pp.83-92, 1996.

[4] Ohno S., Iizuka A. and Ohta H., Two categories of new constitutive derived from non-linear description of soil contractancy, Journal of JSCE, Vol.9, pp.407-414, 2006.

[5] Mualem, Y.: A new model for predicting the hydraulic conductivity of unsaturated porous media, Water Re-sources Research, Vol.12, No.3, pp.514-522, 1976.

[6] Van Genuchten: A closed-form equation for predicting hydraulic of unsaturated soils, Soil Science Society American Journal, Vol.44, pp.892-898, 1980.

[7] Kawai, K., Wang, W. and Iizuka, A.: The expression of hysteresis appearing on water characteristic curves and the change of stresses in unsaturated soils, Journal of applied mechanics, Vol.5, pp.777-784,2002. Kimura S., Journal Paper Title, J. of Computer Science, Vol. 1, Issue 2, 1987, pp. 23-49.

[8] Sugii T. and Uno T.: Modeling the New Moisture Characteristic Curve, Journal of JSCE, pp.130-131, 1995.

[9] Honda M., Iizuka A., Ohno S. Kawai K. and Wang W.: A study of the evaluation method for deformation characteristic of compacted soil, Journal of JSCE, Vol.40, No.2, pp.99-110, 2000.

[10] Japan Road Association,: Roadway Workers - Fill Construction Guidelines, 2010.

[11] Japan Meteorological Agency : http://www.jma.go.jp/jma/index.html.